Frontiers in Health Informatics ISSN-Online:2676-7104
www.healthinformaticsjournal.com
2024; Vol 13: Issue 3
Open Access

Machine Learning Based Identification Of Covid-19 From Lung Segmented Ct Images Using Radiomics Features

Dr. M. Venkatesh[1], T Lakshmi Surekha[2], Dr. P. Neelima[3], P Katheeja Khanam4,Dr. M. Sunil Kumar[5], Dr. D. Ganesh[6]

[1]Associate Professor & HoD, Department of AIML, Aditya University, Surampalem, India.
magantivenkatesh16jan1984@gmail.com

[2]Assistant Professor, Department of Information Technology, Velagapudi Ramakrishna Siddhartha Engineering college (Deemed to be University, Vijayawada
lakshmisurekha@vrsiddhartha.ac.in

[3]Assistant professor, Department of CSE, School of engineering and technology Spmvv, Tirupathi, AP, India
neelima.pannem@gmail.com

[4]Assistant Professor, Department of CSE, School of Computing, Mohan Babu University, (erstwhile Sree Vidyanikethan Engineering College), Tirupathi, AP, India,
aamnakhan521@gmail.com

[5]Professor, Department of CSE, School of Computing, Mohan Babu University, (erstwhile Sree Vidyanikethan Engineering College), Tirupathi, AP, India,
sunilmalchi1@gmail.com

[6]Associate Professor, Department of CSE, School of Computing, Mohan Babu University, (erstwhile Sree Vidyanikethan Engineering College),
dgani05@gmail.com

Cite this paper as: M. Venkatesh, T Lakshmi Surekha,P. Neelima, P Katheeja Khanam, M. Sunil Kumar,D. Ganesh (2024) Machine Learning Based Identification Of Covid-19 From Lung Segmented Ct Images Using Radiomics Features.*Frontiers in Health Informatics, 13* (3), 8546-8557

ABSTRACT

This study article seeks to present a useful tool for doctors to use with deep learning architectures in order to aid in the diagnosis of COVID-19, which has recently surged on a global scale. The examination of medical pictures, namely chest CT images, is the main basis for the automated diagnosis of COVID-19. The small air sacs called alveoli are damaged and the regular functioning of the lungs is affected by this COVID-19. Chest computed tomography (CT) scans are more important for diagnosing patients with severe infections and for screening for COVID-19 immediately prior to specific emergency surgeries and treatments. Radiologists' visual interpretation of chest CT scans has been the gold standard for diagnosis up until now, however it can be inaccurate. To start, diagnosing with a chest CT, which holds hundreds of slices, takes time. The next example is COVID-19, a lung illness that causes a wide range of pneumonia types. Based on the radiomics features of the pre-processed chest CT images, this research aims to detect anomalies and diagnose the severity of COVID-19. This information is useful for differentiating between the usual opaque area, GGOs, and the high intensity area, which contains things like blood vessels and other types of consolidations. In comparison to current qualitative evaluation methods, our

methodology (classification of chest CT images utilising radiomic characteristics for COVID-19 diagnosis using neural network) can reduce subjective variability and increase diagnostic efficiency.

Keywords: *COVID 19, chest CT, radiomics, GGO's, classification, neural network*

1. INTRODUCTION

The newly identified SARS-COV-2 virus causes the infectious condition known as coronavirus (COVID-19). Among the many RNA virus families, this coronavirus is a particularly dangerous one for both humans and other animals. Those who contract this virus will feel mild to moderate respiratory symptoms. People with preexisting conditions, such as heart disease, diabetes, lung disease, or cancer, may experience severe consequences. When it comes to diagnosing COVID-19, there are two major broad groups to consider. Both the laboratory-based technique and chest/thoracic radiography fall under this category. Despite negative results from reverse transcriptase polymerase chain reaction (RT-PCR) tests, COVID-19 can now be diagnosed using chest CT imaging alone. A low viral RNA concentration in the sample, an absence of necessary cellular components, or incorrect acid extraction from the sample are all potential causes of RT-negative PCR test findings.

Until recently, there was a dearth of data demonstrating the validity and efficacy of chest CT scans for the diagnosis of COVID-19 in asymptomatic individuals. It is considered that chest CT has the necessary properties to detect asymptomatic infections for which RT-PCR results were negative, according to the little literatures [1, 2]. The diagnosis of COVID-19 relies heavily on another type of CT scan, the thoracic CT scan. Thoracic CT is the gold standard for diagnosing COVID-19 because of its great sensitivity. The X-rays used in a CT scan must travel through the patient's thoracic region before they can be detected by radiation detectors. These images are then used to recreate the patient's anatomy. If patients with viral lung infections are identified early on, they may not need to be admitted to critical care units, where the condition often has more severe consequences.

The use of artificial intelligence (AI) in computer-assisted diagnosis of SARS-COV-V2 virus infection and its related symptoms was extremely important. Due to its high detection accuracy and low misclassification, AI has been widely considered and used in biomedical investigations since its prominence. Artificial intelligence can be employed to detect patterns in CT scans during the COVID-19 diagnostic process. Features indicating the anomalies were automatically identified from the CT images and utilised for further analysis using AI in the process of focused region segmentation and acquiring refined components in chest tomography images. A large body of recent research has recommended AI-based methods for detecting COVID-19 and differentiating it from other lung diseases and community pneumonia.

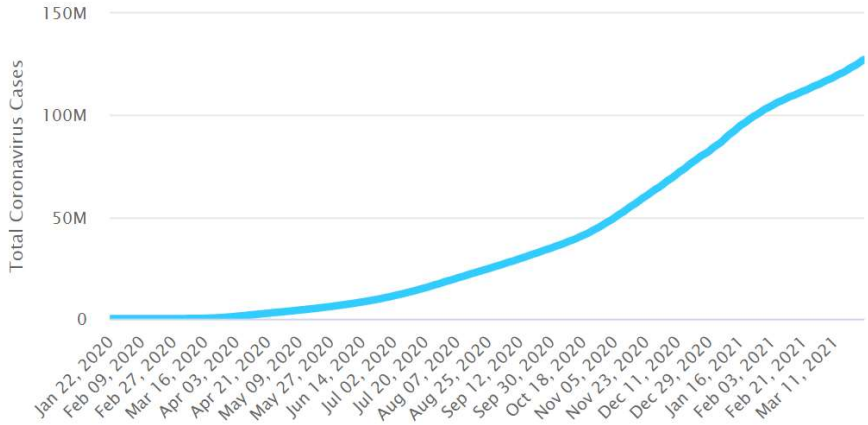

Fig. COVID-19 cases reported every two week by the WHO Region (Source: [3])

The COVID-19 diagnosis process made use of Machine Learning algorithms (ML), a branch of artificial intelligence, which taught the algorithms how to accurately extract relevant information from biomedical images and provide a diagnosis. Among the many types of machine learning algorithms, "deep learning" is most known for its emphasis on building and training deep neural structures that may effectively reveal previously unseen patterns in otherwise complicated data. In recent times, bio-medical image processing has made use of Deep Learning (DL) algorithms such as belief networks (DBN), Deep Neural architectures (DNN), and convolutional networks (CNN), which, when compared to their forebears, the machine learning algorithms, produce superior results. Machine learning and deep learning algorithms, in particular, are playing an increasingly important role in the ongoing effort to contain the COVID-19 pandemic, as well as in the diagnostic and treatment processes. The genetics of SARS-CoV-2 proteins was the focus of recent study that used deep learning algorithms to forecast potential new medication combinations. In order to forecast the onset of a disease in a certain community, its transmission route, and its effects, complicated deep neural architectures were trained using the massive amounts of COVID-19 data and COVID-19-related data retrieved from social networks. Combining computer vision techniques with deep learning algorithms allowed us to track the movement of crowds in public spaces and identify the infected individual.

In order to help doctors control and prevent the spread of the pandemic sickness, an effective automated diagnostic method is needed. It is also clear that standard laboratory testing takes more time, and that even a network of fully-stocked labs cannot handle a heavy workload. Consequently, in urgent and life-threatening circumstances, bio-medical imaging, particularly CT scans, have proven a quick and dependable way to diagnose COVID-19. Estimating the volume of ground glass opacity (GGO), consolidations, and grey patterns in CT images is the main emphasis of COVID-19 analysis. Estimates allow one to ascertain the degree or severity of infection. Chest computed tomography (CT) image segmentation for COVID-19 diagnosis has been the subject of several recent research studies. Segmenting the lungs from the chest CT scans is an important first step in most methods. Prior to performing a Covid-19 severity analysis, it is necessary to identify the lung region in order to extract features. The complicated form of the lung region makes it impossible for object detection techniques to detect it. There is a larger probability of incorrect detections and more work involved in analysing a large volume of CT scan pictures. Therefore, it is crucial to employ automated segmentation of the RoI or lung nodules using the key markers included in the high resolution CT scans. Automated segmentation helps doctors make better diagnoses by focussing on specific regions of interest (ROIs) within CT scans rather than the entire images. Lung area segmentation made use of elementary and fundamental image processing methods, such as morphological

operations, active shape models, and clustering algorithms. The end-to-end learning architecture provided more accurate segmentation than the hand-crafted feature-based approach. U-Net and similar encoder-decoder architectures are used for biomedical picture segmentation most of the time. Using several datasets to assess a segmentation model's efficacy is a big challenge in lung segmentation. Unfortunately, there are currently no benchmark models that can be used as a main point of reference for segmentation.

Radiomics is a non-invasive machine learning technique that efficiently transforms multi-dimensional biomedical images into features that can best describe the nature and components (that are not visible to the naked eye) present in the images by extracting a large number of beat representational features. The accuracy of predicting different types of carcinoma, such as lung, rectal, and non-neoplastic illnesses, and the potential benefits of radiomics in improving the diagnostic process have been highlighted [10–13]. Radiomics characteristics retrieved from chest CT for rapid and accurate diagnosis of COVID-19 pneumonia are not yet supported by a large enough data set.

Classifying CT images of COVID-19 infected individuals from normal and infected individuals with other prevalent lung infections following segmentation of the lungs is the goal of this investigation[27-28].

the CT scans of gion. After extracting radiomics features (such as shape and texture) from CT image slides, UNET architecture was employed for lung segmentation. A back propagation algorithm-trained neural network was used for classification.

2. LITERATURE SURVEY

Automated delineation of various diseased organs in biomedical pictures is becoming a crucial component of computer-assisted diagnosis. Semantic segmentation architectures, such as UNet, and other deep learning methods were becoming increasingly important in automated organ delineation. Semantic segmentation of organs of interest from CT scans, including the lungs, is addressed in this section using a variety of deep learning models. The benefit of employing dilated convolutional layers, which extracted global information from the input images, was examined in a research article [4][25]. Improved overall delineation accuracy was achieved by the enlarged convolutional layers' ability to efficiently understand the organ's architecture. Because lung illness alters tissue density, leading to fluctuations in CT image intensity, lung segmentation from medical pictures presents a significant difficulty. Hence, intensity-based segmentation methods are untrustworthy. The diseased lung was automatically segmented from the CT picture using graph search in [5][24]. An objective function constructed from the combined intensity, gradient, smooth border, and rib region meta-information is included in the graph search approach. One approach to segmenting various organs from chest CT scans using an adversarial network called UNet-GAN was suggested [6][22]. The goal was to aid in radiation treatment planning. The generators in this case were a collection of U-Net models, while the discriminator was a fully convolutional network. Using its training data, the generator network can produce a segmentation map for an input image. It learns the end-to-end process of mapping CT images to multi-organ segmentation images during model training [20][26].

Lungs were segmented from Electrical Impedance Tomography (EIT) images using the UNET architecture in a recent work [7][19][21]. The trained U-Net could detect and separate variations in conductivity in EIT pictures even when given no training data. Prior work attempted to segment the lungs in each CT slice using thresholding techniques; this enhanced segmentation by dividing the right and left halves of the lung relative to the anterior junction line [8]. There was a suppression of the diaphragm region and an elimination of the bronchi and trachea during the post-processing stages. It is necessary to overcome obstacles generated by bronchi, veins, and arteries

that seem closer to the chest tissues in order to properly segment the lungs from the Low Dose Tomographic (LDCT) pictures. Consequently, in order to preserve the information and details accessible in the lung region, the segmentation approach should consider the spatial link between the different components of the lungs. Lung segmentation from LDCT was first accomplished using the Linear Combination of Discrete Gaussians (LCDG) in [9], and subsequently, the segmentation was fine-tuned using the Markov-Gibbs-random-field model (MGRF). Disease progression can be predicted and studied using radioomics characteristics, which comprise efficient and high-dimensional representational features [18] obtained from statistical and textural data as well as quantitative analysis of greyscale picture pixels [23].

METHODOLOGY

To eliminate pepper and salt noise and maintain edge preservation, the CT images undergo pre-processing with a median filter. As a median filter, a 3x3 square filter is utilised. The mean filter is commonly employed to eliminate noise from biomedical pictures; however, it has a blurring effect and impacts lung segmentation and GGO detection in general. Since noise is not a major concern with CT images, we used a median filter to eliminate spike spots and smooth the image; this solved the problem.

The goal is to construct a mathematical model M using the encoder-decoder architecture and run experiments to find the best collection of hyper-parameters, given a set of pictures X ∈ R^(n_r,n_c) and a corresponding binary mask Y ∈{0,1}^(n_r,n_c). To train the model and reduce overall loss, we use the provided photos. Then, we use a validation set to verify the model's generalisation ability. In general, the goal of training is to find a point in the weight space where the model produces an output Yˆ_test that is nearly identical to the predicted or target output Y_test, given an input X_test. When the test samples used for performance analysis adhere to the following criteria; X_(test)∩X=∅, the testing will be more dependable.

With a pixel size of 0.5 mm x 0.5 mm, the image scale in the slice was standardised using bicubic resampling. A number of statistical features, including intensity-based ones, gray-level co-occurrence matrix (GLCM) features, and gray-level run-length matrix (GLRLM) features, were created using both the original CT picture and the adjusted image. We normalise the radiomic properties to z-scores using the parameters computed in the training set.

3.1 Modeling

The current study makes use of radiomic markers that are highly correlated with the categorisation of COVID-19 patients and those who do not have the virus. Deep learning-based approaches have shown to be more efficient than the laborious human procedure of segmenting aberrant or infected CT images. Our experimental results also show that radiomics is a viable technique for diagnosing COVID. Because there were no significant statistical differences in the radiomics features obtained from the manual segmentation of the lung region among radiologists, the correctness of the infection image analysis in this study could be guaranteed.

This study used the back-propagation neural network (BPNN) classifier to evaluate how well radiomics features could classify COVID-19. The BPNN was able to successfully distinguish between the two input classes because to the differentiable activation function that received the outputs from the network nodes and the back propagation technique that updated the weights connecting the internal network nodes after each training session. Because of its superior capacity to build complex decision surfaces in a feature space with many dimensions, BPNN was

selected as the classifier. Some studies have even shown that BPNN output is quite similar to Bayesian posterior probability results. This matters because Bayesian classifiers achieve the best accuracy (i.e., minimum mis-classification) for a specific distribution of feature data. Like other non-parametric approaches to pattern classification, BPNN performance cannot be predicted in advance. In addition to the learning parameter, other BPNN parameters include the training sample volume, the hidden layer node count, and the number of hidden layers.

We may establish a limit (m) on the number of training samples needed to achieve a specific level of performance over a set of test samples with the same probability distribution as the training samples based on the work of Baum and Haussler [17]. When a neural network with N nodes and W parameters is trained using m training samples, it may be expected that a fraction equal to 1- $\epsilon/2$ of the test samples would be properly identified. One possible mathematical definition of m is

$$m \geq O\left(\frac{W}{\epsilon}\log\frac{N}{\epsilon}\right)$$

In order to maintain an error rate of less than 10% when categorising the test samples, the number of training samples was maintained to be around 10 times the number of weights in the network. A standard three-layer network with 100 nodes per layer requires over 10,000 training data. Making so many images is just not doable. Thankfully, this bound does not rule out the prospect of building an effective classifier with fewer training instances, as other research have demonstrated. Using data augmentation techniques, new training data samples were created from existing training pictures. Experiments were conducted on both the dataset with and without the augmentation.

We don't have any theory to back up our claims about how many hidden nodes should be used in a single hidden layer network. One way to get this value to its maximum potential is to experiment with different numbers of hidden nodes in the network and pick the one that works best. A cross validation method was employed to adjust the hyperparameter values of the network. The associated radiomics investigations [14–16] served as the basis for randomly dividing the segmented photographs into two datasets, one for training and the other for testing, with a ratio of 80:20. Once the classification model was obtained from the training dataset, images from the test datasets were used as a validation dataset. Because of this, the approach given in this study could be checked by another party.

4. EXPERIMENTS AND RESULTS

The results obtained by the suggested method are detailed in the next part. This section covers the COVID-19 dataset, experimental setup, quantitative and qualitative results, analysis of failures, and discussion.

4.1 Dataset

An open-source SARS-CoV-2 CT scan dataset contains 2482 scans; 1252 of these scans tested positive for SARS-CoV-2 infection (COVID-19), while 1230 scans were taken from individuals who did not have the virus. Patients in Sao Paulo, Brazil, who were actually seeking medical attention provided the data. Between male and female patients, there were no discernible differences in demographic data ($p<0.05$). The proportion of patients whose SARS-CoV-2 infection was categorised as early, intermediate, or late according to the interval between the start

of symptoms and the admission CT scan. We utilised a data augmentation strategy to boost the quantity of training samples because it is essential for a model to be trained correctly.

4.2 Experimental setup and results

After applying the trained U-NET architecture to the pre-processed pictures, the lung area was used to extract radiomics features. During training, data augmentation is used to make the network more resilient. This involves slightly changing the signal strength of the images, adding noise, rotating, skewed, warping, and randomly scaling them. When training neural networks, their initial values for parameters like learning rate, bias, and weight are utilised. beginning with a beginning value, it iteratively updates the weight to determine its leaning angle. There is a lot of complexity and time required for training a neural network.

The difficulty with relying solely on sensitivity and specificity metrics to evaluate a model is that they are very sensitive to the threshold value that is used to change the model's performance. When dealing with a binary classification issue, it is important to keep in mind the false positive rate as well as the false negative rate as potential forms of error. To get a more complete picture of a model, it's best to use metrics that combine FPR and FNR when evaluating it. By plotting the true positive rate (y-axis) against the false positive rate (x-axis) for a variety of thresholds from zero to one, the Receiver operating characteristic (ROC) shows how the two rates interact and is thus a popular tool for many strategies.

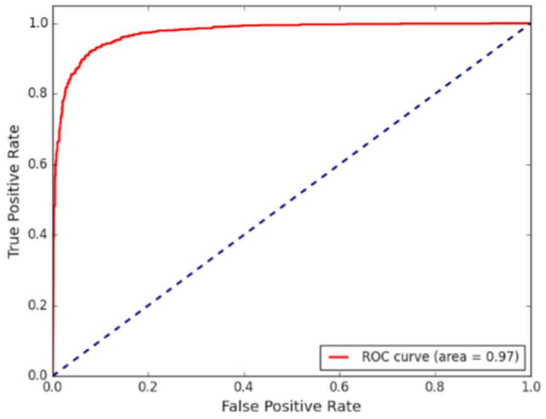

Fig 4.2(a): Reciever Operating Characteristic (ROC) of Neural Classifier

A receiver operating characteristic (ROC) curve was utilised to evaluate the radiomics, CT image effectiveness, and classification abilities of the models. We determined the specificity, accuracy, and sensitivity using the area under the curve (AUC) method. Decision curve analysis (DCA) and calibration curves were constructed to evaluate the models' accuracy and clinical utility. By utilising the cut-off value in the training set, which is determined by the maximum index of each model for ROC analysis, the confusion matrix, specificity, sensitivity, and accuracy in both the training and test cohorts were approximated. Both the average optimism and the optimism-adjusted AUC show that the feature-based model is very reliable. It was determined how well the classifier worked by looking at its sensitivity, specificity, and accuracy. The ROC curve was also used for performance evaluation. To test how well the classifier identified real COVID images from potential false positives, ROC analysis was employed. The classification model's output values were used to calculate the areas

under the ROC curve.

Table 4.2(a): Dataset training/testing with and without data augmentation

DATA	NO AUGMENTATION		WITH AUGMENTATION	
	COVID-19	Non-COVID-19	COVID-19	Non-COVID-19
Training	760	710	3040	2850
Test	492	520	504	530
total	1252	1230	3544	3380

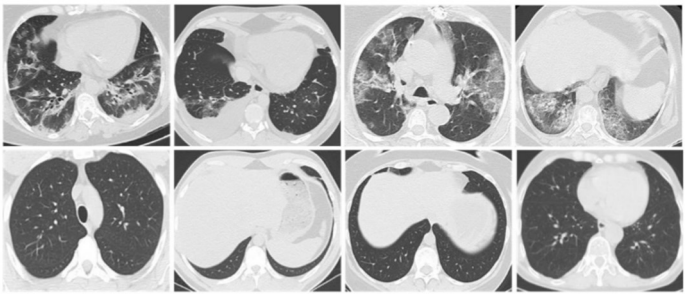

Fig 4.2(b): The first row of samples belongs to the covid-19 cases, whereas the second row belongs to the non-COVID instances.

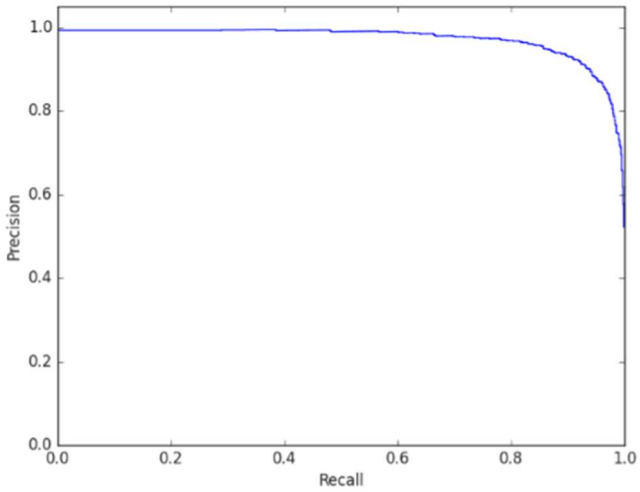

Fig 4.2(c): The test set's precision-recall curve

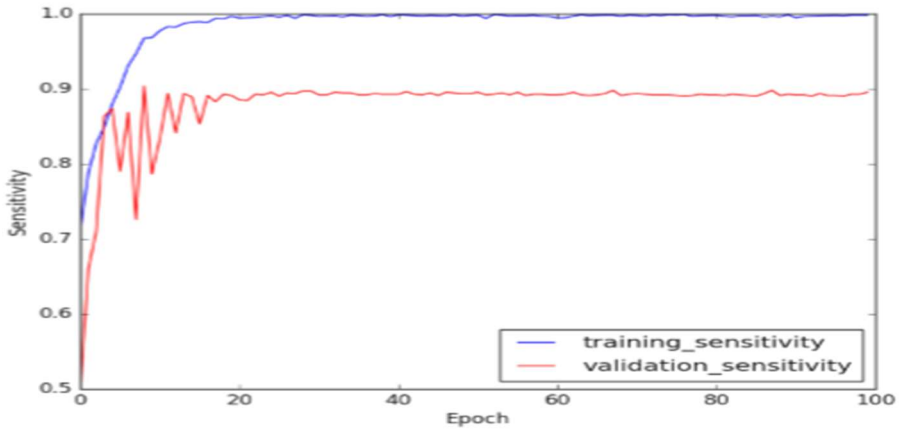

Fig 4.2(d): Model sensitivity during training and validation

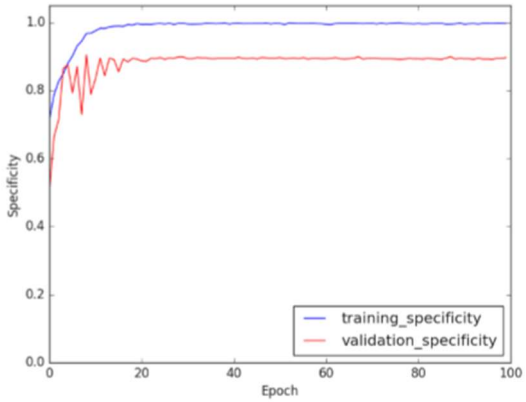

Fig 4.2(e): Model specificity during training and validation

One way to measure how well a classifier is doing is to look at its ROC curve, which contains common performance indicators like specificity, sensitivity, and accuracy. For different threshold levels, the sensitivity and false positive rate are plotted to create ROC curves. The performance of the classifier can be summarised by calculating the area under the ROC curves. You can get these numbers using the following formula.

$$\text{Sensitivity} = \frac{\text{TP}}{\text{TP+FN}} \quad , \qquad \text{Eq.4.2 (a)}$$

$$\text{Specificity} = \frac{TN}{TN+FP} \quad , \qquad \text{Eq.4.2 (b)}$$

$$\text{Accuracy} = \frac{TP+TN}{TP+FP+TN+FN} \quad , \qquad \text{Eq.4.3 (c)}$$

A true positive (TP), negative (TN), false positive (FP), or false negative (FN) label is used to indicate a result that is not true.

Table 4.2(b): Summary of scores of sensitivity and specificity for various threshold values.

Threshold	Sensitivity	Specificity	F1 score
0.1	0.85 ± 0.002	0.96 ± 0.001	0.90 ± 0.001
0.2	0.87 ± 0.002	0.95 ± 0.001	0.90 ± 0.001
0.3	0.89 ± 0.002	0.94 ± 0.001	0.91 ± 0.001
0.4	0.89 ± 0.002	0.93 ± 0.001	0.91 ± 0.001
0.5	0.90 ± 0.002	0.93 ± 0.001	0.91 ± 0.001
0.6	0.89 ± 0.002	0.93 ± 0.001	0.91 ± 0.001
0.7	0.89 ± 0.002	0.94 ± 0.001	0.91 ± 0.001
0.8	0.87 ± 0.002	0.95 ± 0.001	0.90 ± 0.001
0.9	0.85 ± 0.002	0.96 ± 0.001	0.90 ± 0.001

Machine learning correctly identifies these photos as COVID instances, and the number of COVID positive cases, according to the RT-PCR report, is TP. Unfortunately, the machine learning algorithm incorrectly labels a small proportion of individuals as positive, even though they are actually afflicted with ordinary flu or fever and do not have COVID. The machine learning method correctly identifies these modules as non-COVID cases, and the pathology report indicates that there are TN of them. Ground Glass Opacity (GGO) was absent from most slices in the training set. Using the segmentation model's completely linked dense layers, we were able to obtain features using the already trained feature extraction block. Then, we used these features to make a binary choice.

5. CONCLUSION

Evaluation of machine learning architectures for COVID-19 prediction using chest CT scans was the primary goal of this study. In order to aid doctors in the diagnosis and treatment of COVID-19, a neural network was built using RADIOMICS features collected from the segmented pictures. To boost the amount of training samples, data augmentation techniques were used in conjunction with the public dataset during model training. The specificity, sensitivity, precision-recall, and ROC curves of the model were all experimentally evaluated. Using CT scans and matching lung mask images, the UNET segmentation model was trained and evaluated using comprehensive pictures spanning the early, medium, and late phases of COVID-19 disease.

REFERENCES

1. Fang Y, Zhang H, Xie J, Lin M, Ying L, Pang P, et al. Sensitivity of chest CT for COVID-19: comparison to RT-PCR. Radiology 2020; 296: E115–7.
2. Inui S, Fujikawa A, Jitsu M, Kunishima N, Watanabe S, Suzuki Y, Motoyuki J, et al. Chest CT findings in cases from the cruise ship diamond princess with Coronavirus disease (COVID-19). Radiology 2020; 2: e200110.
3. https://www.worldometers.info/coronavirus/worldwide-graphs/
4. Lei Geng, Siqi Zhang, Jun Tong & Zhitao Xiao (2019) Lung segmentation method with dilated convolution based on VGG-16 network, Computer Assisted Surgery, 24:sup2, 27-33

5. Hua, Panfang, Qi Song, Milan Sonka, Eric A. Hoffman, and Joseph M. Reinhardt. "Segmentation of pathological and diseased lung tissue in CT images using a graph-search algorithm." In *2011 IEEE International Symposium on Biomedical Imaging: From Nano to Macro*, pp. 2072-2075.
6. Dong, Xue, Yang Lei, Tonghe Wang, Matthew Thomas, Leonardo Tang, Walter J. Curran, Tian Liu, and Xiaofeng Yang. "Automatic multiorgan segmentation in thorax CT images using U-net-GAN." *Medical physics* 46, no. 5 (2019): 2157-2168.
7. Ko, Yen-Fen, and Kuo-Sheng Cheng. "U-Net-based approach for automatic lung segmentation in electrical impedance tomography." *Physiological Measurement* 42, no. 2 (2021): 025002.
8. Armato III, Samuel G., and William F. Sensakovic. "Automated lung segmentation for thoracic CT: impact on computer-aided diagnosis1." Academic Radiology 11, no. 9 (2004): 1011-1021.
9. El-Ba, Ayman, Georgy Gimel'farb, Robert Falk, Trevor Holland, and Teresa Shaffer. "A new stochastic framework for accurate lung segmentation." In International Conference on Medical Image Computing and Computer-Assisted Intervention, pp. 322-330. Springer, Berlin, Heidelberg, 2008.
10. Guiot J, Vaidyanathan A, Deprez L, et al. Development and validation of an automated radiomic CT signature for detecting COVID-19. medRxiv. 2020.
11. Liu Z, Zhang XY, Shi YJ, et al. Radiomics analysis for evaluation of pathological complete response to neoadjuvant chemoradiotherapy in locally advanced rectal cancer.
12. Chen BT, Chen Z, Ye N, et al. Differentiating peripherally-located small cell lung cancer from non-small cell lung cancer using a CT radiomic approach.
13. Liu Y, Dong D, Zhang L, et al. Radiomics in multiple sclerosis and neuromyelitis optica spectrum disorder. Eur Radiol. 2019; 29:4670–7.
14. J. Zhou, H. Tan, Y. Bai, J. Li, Q. Lu, R. Chen, M. Zhang, Q. Feng, M. Wang, Evaluating the HER-2 status of breast cancer using mammography radiomics features, Eur. J. Radiol. 121 (2019) 108718.
15. R.T. Leijenaar, M. Bogowicz, A. Jochems, F.J. Hoebers, F.W. Wesseling, S. H. Huang, B. Chan, J.N. Waldron, B. O'Sullivan, D. Rietveld, Development and validation of a radiomic signature to predict HPV (p16) status from standard CT imaging: a multicenter study, Br. J. Radiol. 91 (1086) (2018) 20170498.
16. H.-Y. Tsao, P.-Y. Chan, E.C.-Y. Su, Predicting diabetic retinopathy and identifying interpretable biomedical features using machine learning algorithms, BMC Bioinformatics 19 (9) (2018) 283.
17. E.B. Baum and D. Haussler, What size net gives valid generalization?, *Neural Computation*, vol. 1, no. 1, pp. 151-160, 1989.
18. Kumar, M. Sunil, et al. "Advancements in Heart Disease Prediction: A Comprehensive Review of ML and DL Algorithms." 2023 3rd International Conference on Technological Advancements in Computational Sciences (ICTACS). IEEE, 2023.
19. Reddy, B. Ramasubba, et al. "Medical Image Tampering Detection using Deep Learning." 2024 5th International Conference on Smart Electronics and Communication (ICOSEC). IEEE, 2024.
20. Burada, S., Manjunathswamy, B. E., & Kumar, M. S. (2024). Early detection of melanoma skin cancer: A hybrid approach using fuzzy C-means clustering and differential evolution-based convolutional neural network. Measurement: Sensors, 33, 101168.
21. Gandikota, Hari Prasad, S. Abirami, and M. Sunil Kumar. "Bottleneck Feature-Based U-Net for Automated Detection and Segmentation of Gastrointestinal Tract Tumors from CT Scans." Traitement du Signal 40.6 (2023).
22. Rafee, Shaik Mohammad, et al. "2 AI technologies, tools, and industrial use cases." Toward Artificial General Intelligence: Deep Learning, Neural Networks, Generative AI (2023):

23. Gandikota, Hari Prasad, S. Abirami, and M. Sunil Kumar. "Bottleneck Feature-Based U-Net for Automated Detection and Segmentation of Gastrointestinal Tract Tumors from CT Scans." Traitement du Signal 40.6 (2023).
24. Reddy, A. Rama Prathap, et al. "The ANN Method for Better Living's Method of using Artificial Neural Networks to Predict Heart Attacks Caused by Anxiety Disorders." 2023 3rd International Conference on Advance Computing and Innovative Technologies in Engineering (ICACITE). IEEE, 2023.
25. Padmavathi, Bvv, et al. "Implementation of Speech Processing Techniques for Human Emotion Recognition." 2024 International Conference on Computational Intelligence for Green and Sustainable Technologies (ICCIGST). IEEE, 2024.
26. Bindu, GB Hima, et al. "Comparison of Novel Machine Learning Algorithms for Predicting Chronic Renal Disease." 2024 International Conference on Computational Intelligence for Green and Sustainable Technologies (ICCIGST). IEEE, 2024.
27. Ranjan, M. Jaya, et al. "Application of Machine Learning Algorithms to Predict New Mobile Customers." 2024 International Conference on Computational Intelligence for Green and Sustainable Technologies (ICCIGST). IEEE, 2024.
28. Huang Y Q, Liang C-H, He L, Tian J, Liang C-S, Chen X, Ma Z L and Liu Z Y 2016 Development and validation of a radiomics nomogram for preoperative prediction of lymph node metastasis in colorectal cancerJ. Clin. Oncol. 34 2157–64.